

# N-dimensional generalized Hurst-Kolmogorov process and its application to wind fields

P. Dimitriadis<sup>1</sup>, D. Koutsoyiannis<sup>1</sup> and C. Onof<sup>2</sup>

<sup>1</sup>Department of Water Resources and Environmental Engineering, National Technical University of Athens

<sup>2</sup>Department of Civil and Environmental Engineering, Imperial College of London

## Abstract

An N-dimensional generalized Hurst-Kolmogorov stochastic model is presented that can simulate time-varying spatial geophysical fields, consistent with the observed long-term spatial and temporal persistence. The model is tested through some applications based on time-varying wind velocity field.

## 1. Introduction and definitions

Multi-dimensional stochastic processes are advantageous over multivariate ones, in cases where the natural process is observed by images (e.g. produced by satellite, radar) rather than point measurements (e.g. in meteorological stations for rainfall, temperature etc.). We use the methodology followed in Dimitriadis et al. (in publication) where the definitions of 1D stochastic models, as given in Koutsoyiannis (2013) and Dimitriadis and Koutsoyiannis (in publication), is expanded to the LD case. We denote  $\underline{x}(t)$  the continuous space stochastic process that we use to represent the LD natural process, with  $t$  a vector of  $L$  variables, i.e.  $t := (t_1, \dots, t_L)$ , that describe the natural process (e.g.  $t_1$  can be a time variable,  $t_2$  a spatial one etc.). Recorded samples associated with the observed natural process are subject to a spatial or temporal step of sampling  $\mathbf{D} := (D_1, \dots, D_L)$ , often fixed by the observer and a response time  $\Delta := (\Delta_1, \dots, \Delta_L)$  characteristic of the instrument (in fig. 1 the case for a 1D process is shown). Both  $\mathbf{D}$  and  $\Delta$  have the same units as  $t$  (e.g. if  $t_1$  is a temporal variable in seconds then  $D_1$  and  $\Delta_1$  will be measured in seconds as well). To correctly represent the observed natural process with a stochastic one, we have to discretize the latter by including also the values  $\mathbf{D}$  and  $\Delta$ . The two special cases where  $\Delta_i=0$  and  $\Delta_i=D_i$  for a 1D process ( $L=1$ ), are analyzed in Koutsoyiannis (2013), who shows that there are small differences between them. Here, we will focus only in the case  $\mathbf{D}=\Delta>0$ . Also, for simplicity, we assume that  $D_1, \dots, D_L$  have the same magnitude (e.g.  $D_1=1$  s,  $D_2=1$  km etc.) and so, we can use a unique symbol for that magnitude, i.e.  $|\mathbf{D}| = D = \Delta$ . Thus, the discretized stochastic process  $\underline{x}_i^{(\Delta)}$ , for  $D = \Delta > 0$ , can be estimated from  $\underline{x}(t)$  as:

## 2. Definitions (cont.)

$$\underline{x}_i^{(\Delta)} := \frac{\int_{(i_1-1)\Delta_1}^{i_1\Delta_1} \int_{(i_2-1)\Delta_2}^{i_2\Delta_2} \dots \int_{(i_L-1)\Delta_L}^{i_L\Delta_L} \underline{x}(\xi_1, \xi_2, \dots, \xi_L) d\xi_1 d\xi_2 \dots d\xi_L}{\Delta_1 \Delta_2 \dots \Delta_L} \quad (1)$$

where  $i = (i_1, \dots, i_L)$ , with  $i_k \in [1, n_k]$ ,  $\mathbf{i} \in [1, n_1] \times [1, n_2] \times \dots \times [1, n_L]$  denoting the sequent numbers of a specific discretized point of  $\underline{x}$  for each dimension,  $\mathbf{n} = (n_1, \dots, n_L) = (\text{int}(T_1/\Delta_1), \dots, \text{int}(T_L/\Delta_L))$ , the vector of the total number of discretized points in each dimension and  $\mathbf{T} = (T_1, \dots, T_L)$ , the vector of durations (for a time variable) or lengths (for a spatial variable) of  $\underline{x}(t)$ .

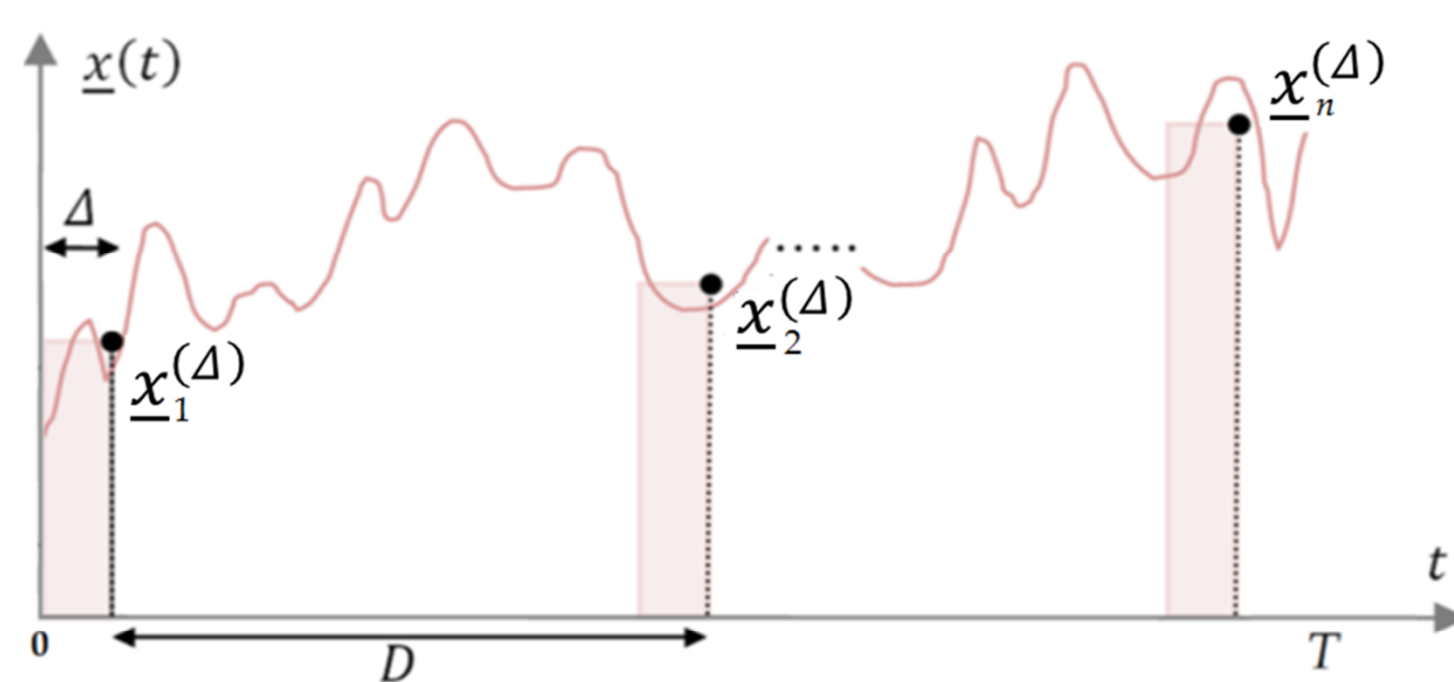


Figure 1: An example of a 1D continue sample of ( $T$ ) duration and the sampling process with sampling frequency ( $D$ ) and instrument response ( $\Delta$ ). We assume that  $t$  is continue and of infinite size.

## 3. Stochastic tools (climacogram)

Table 1: Climacogram definition and expressions for a continuous (true) and a discretized LD process, a common estimator and its expected value.

Type	Climacogram	
continuous space (true)	$\gamma(\mathbf{m}) = \frac{\text{Var} \left[ \int_{t_1}^{t_1+m_1} \dots \int_{t_L}^{t_L+m_L} \underline{x}(\xi_1, \dots, \xi_L) d\xi_1 \dots d\xi_L \right]}{(m_1 m_2 \dots m_L)^2}$	(2)
	where $\mathbf{m} = (m_1, \dots, m_L)$ , with $\mathbf{m} \in \mathbb{R}^+$ , the vector of the scales.	
discretized space	$\gamma_d^{(\Delta)}(\mathbf{k}) = \gamma(\Delta_1 k_1, \dots, \Delta_L k_L)$	(3)
	where $\mathbf{k} = (k_1, \dots, k_L)$ , with $\mathbf{k} \in \mathbb{N}^+$ , the vector of all the dimensionless scales for a discretized process.	
classical estimator	$\hat{\gamma}_d^{(\Delta)}(\mathbf{k}) = \frac{1}{N/K-1} \sum_{i=1}^{N/K} \left( \frac{1}{K} \left( \sum_{r=1}^{K-i} \dots \sum_{r_L=K_L-(i-1)+1}^{K_L} \underline{x}_i^{(\Delta)} \right) - \frac{\sum_{i=1}^{N/K} \underline{x}_i^{(\Delta)}}{N} \right)^2$	(4)
	where $N = n_1 n_2 \dots n_L$ and $K = k_1 k_2 \dots k_L$	
expected value of estimator	$E[\hat{\gamma}_d^{(\Delta)}(\mathbf{k})] = \frac{1-\gamma_d^{(\Delta)}(\mathbf{k})}{1-K/N} \gamma_d^{(\Delta)}(\mathbf{k})$	(5)

Note that the true climacogram can be estimated from the true autocovariance as (expansion of Koutsoyiannis et al. 2010 expression of the 2D case):

$$\gamma(\mathbf{m}) = 2^L \int_0^1 \dots \int_0^1 (1-\xi_1) \dots (1-\xi_L) c(\xi_1 m_1, \dots, \xi_L m_L) d\xi_1 \dots d\xi_L \quad (6)$$

## 4. Stochastic tools (autocovariance and variogram)

Table 2: Autocovariance and variograms definition and expressions for a continue (true) and a discretized LD process, a common estimator and its expected value.

Type	Autocovariance	
continuous space (true)	$c(\tau) = \text{Cov}[\underline{x}(t), \underline{x}(t+\tau)] = \frac{\partial^{2L} (c_{11} \dots c_{LL}) \gamma(\tau)}{2^L \partial \tau_1 \partial \tau_2 \dots \partial \tau_L^2}$	(7)
	where $\tau = (\tau_1, \dots, \tau_L)$ , with $\tau \in \mathbb{R}$ , the vector of lags of the continue process.	
discretized space	$c_d^{(\Delta)}(j) = \text{Cov}[\underline{x}_j^{(\Delta)}, \underline{x}_{j+\mathbf{j}}^{(\Delta)}] = \frac{\Delta^{2L} (c_{11} \dots c_{LL}) \gamma(\mathbf{j})}{2^L \Delta_1^2 \Delta_2^2 \dots \Delta_L^2}$	(8)
	where $\mathbf{j} = (j_1, \dots, j_L)$ , with $\mathbf{j} \in \mathbb{Z}$ , the vector of lags of the discretized process.	
classical estimator	$\hat{c}_d^{(\Delta)}(j) = \frac{1}{\zeta(j)} \sum_{i=1}^{N/n_1-j_1} \dots \sum_{i_L=1}^{N/n_L-j_L} \left( \underline{x}_i^{(\Delta)} - \frac{\sum_{i=1}^{N/n_1-j_1} \dots \sum_{i_L=1}^{N/n_L-j_L} \underline{x}_i^{(\Delta)}}{N} \right) \left( \underline{x}_{i+\mathbf{j}}^{(\Delta)} - \frac{\sum_{i=1}^{N/n_1-j_1} \dots \sum_{i_L=1}^{N/n_L-j_L} \underline{x}_i^{(\Delta)}}{N} \right)$	(9)
	where $\zeta(j)$ is usually taken as: $N$ or $N-1$ or $\prod_{k=1}^L (n_k - j_k)$ .	
expected value of estimator	$E[\hat{c}_d^{(\Delta)}(j)] = \frac{1}{\zeta(j)} (c_d^{(\Delta)}(j) \prod_{k=1}^L (n_k - j_k) + \frac{1}{N} \gamma(\mathbf{j}) - j \gamma(\mathbf{j}) - \frac{\prod_{k=1}^L (n_k - j_k)^2}{N} \gamma((n - \mathbf{j})\mathbf{A}))$	(10)
	where $\mathbf{j} = j_1 j_2 \dots j_L$ .	
	Variogram	
continuous space (true)	$v(\tau) = c(0) - c(\tau)$	(11)
discretized space	$v_d^{(\Delta)}(j) = c_d^{(\Delta)}(0) - c_d^{(\Delta)}(j)$	(12)
expected value of estimator	$E[\hat{v}_d^{(\Delta)}(j)] = E[\hat{c}_d^{(\Delta)}(0)] - E[\hat{c}_d^{(\Delta)}(j)]$	(13)

## 5. Generalized HK stochastic model (gHK)

Table 3: Autocovariance for a 2D spatial continue and discretized gHK (or Cauchy type for the 1D case) process (eq. 7 and 8) and the 1D gHK climacogram. Note that solution of eq. 6 for the 2D climacogram is not a closed expression.

Type	Generalized HK stochastic model	
Autocovariance (true, continuous space)	$c(\tau_1, \tau_2) = \lambda (\sqrt{\tau_1^2 + \tau_2^2} / q + 1)^{-b}$	(14)
	with $b = 4 - 4H$	
Autocovariance (discretized space)	$c_d^{(\Delta)}(j_1, j_2) = \frac{\Delta^2 [(j_1 j_2)^2 \gamma(j_1, j_2)]}{2^2 \Delta_1^2 \Delta_2^2}$	(15)
	with $\frac{\Delta^2 \gamma(j_1, j_2)}{\Delta_1^2 \Delta_2^2} = (j_1 + 1) \gamma(j_1 + 1) + (j_2 - 1) \gamma(j_2 - 1) - 2j_1 j_2 \gamma(j_1, j_2)$	
1D climacogram (continuous and discretized space)	$\gamma(m) = \frac{2\lambda [(m/q + 1)^{2-b} - (2-b)m/q - 1]}{(1-b)(2-b)(m/q)^2}$	(16)
	with $\gamma(0,0) = \lambda$ and for $q=0$ : $\gamma(0,0) \rightarrow \infty$	

To fit an observed climacogram, we first use the estimated value of eq. 13 (described in eq. 5) for the 1D case, replacing  $m$  with  $\sqrt{m_1^2 + m_2^2}$ , to have a first approximation of the fitted parameters. Then, we use eq. in Tables 1 and 2, for the 2D case, to find the best fitted parameters based on a target value (sum of squares of differences between observed and estimated values) for each stochastic tool (climacogram, autocovariance and variogram). Note that we do not use all possible scales and lags but rather a selection of them logarithmically spaced.

## 6. Simulated MHD turbulence in the solar wind

Here, we apply a combination of Markovian and gHK models to a 2D spatiotemporal numerical simulation of freely decaying MHD turbulence in the solar wind. This simulation is performed by ESA and based on recent observations from Cluster spacecraft (Perri et al., 2012). We use the animation video provided by J. Donelli of NASA: <http://www.youtube.com/watch?v=BNdMEucVsX0>

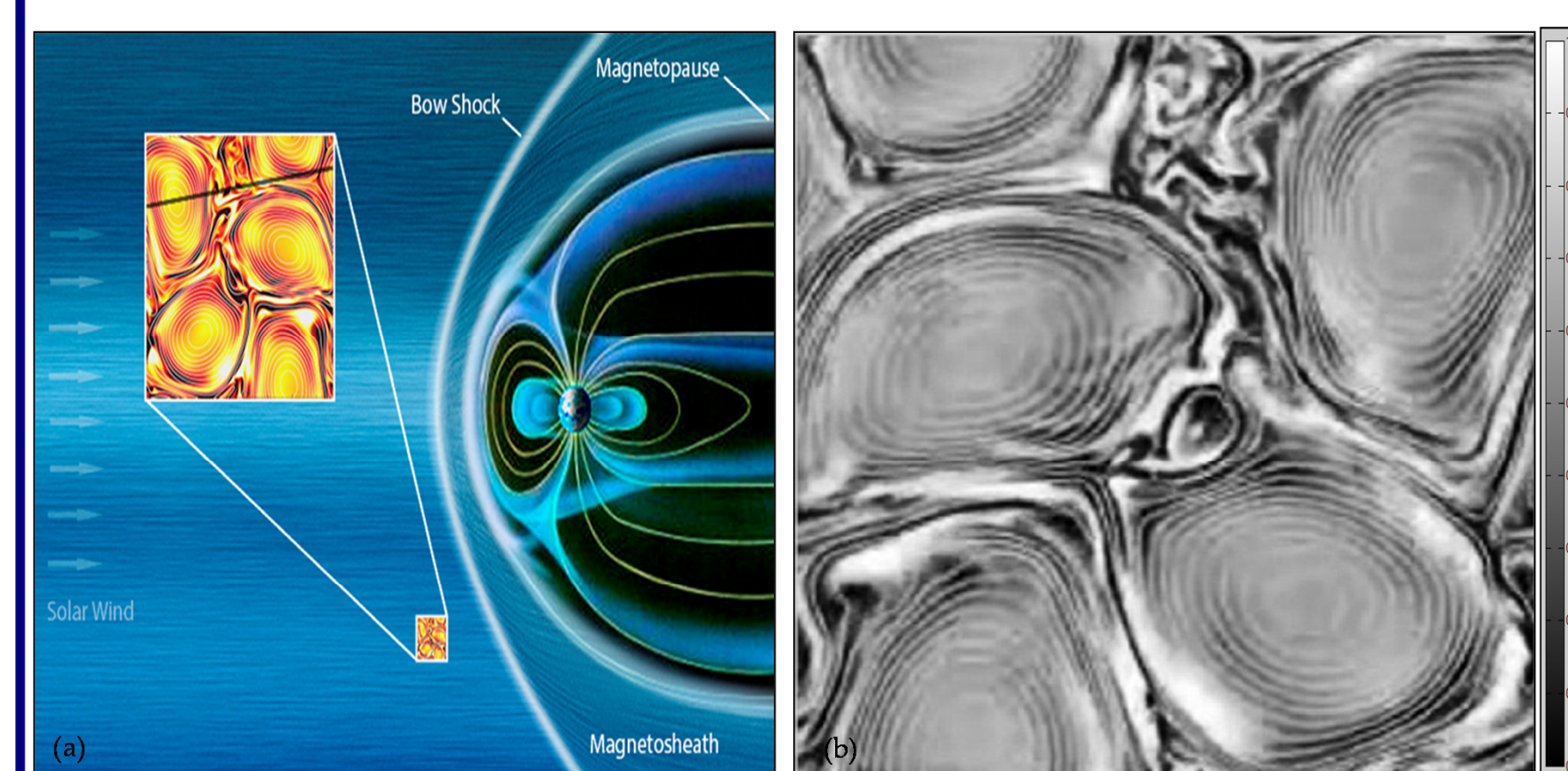


Figure 2: The image on the right (b) represent the strength of the magnetic field  $G$  (with 4.8 nT the darkest grayscale shades and 5.2 nT the white ones) at the last frame of the simulation. It is perpendicular to the interplanetary magnetic field and to the direction of flow of the solar wind (as shown in (a)). Source: <http://sci.esa.int/cluster/51231-turbulent-eddies-may-warm-the-solar-wind/>.

## 7. Simulated MHD turbulence in the solar wind (cont.)

The parameters are estimated as:  $\lambda=0.04\mu$  (nT),  $q=8v$  (nT) and  $b=1.5$  ( $H=0.6$ ), where  $\mu=0.4G+4.8$  (nT) and  $v=13,000$  km (earth's diameter).

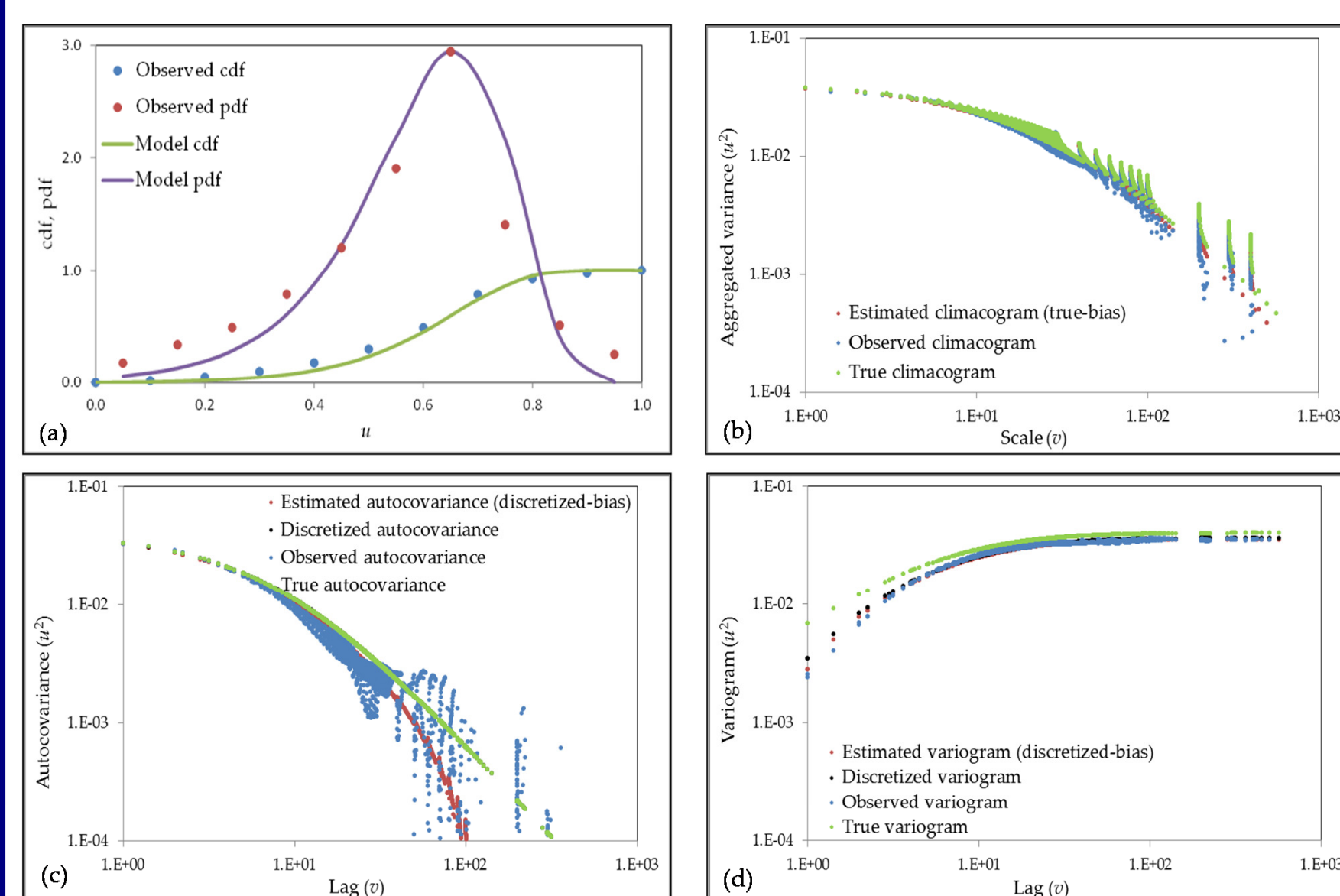


Figure 3: Fitted Gompertz negatively skewed cdf and pdf (a), climacograms (b), autocovariances (c) and variograms (d) of the MHD turbulence in the solar wind simulation image of fig. 2b.

## 8. Hurricane wind speed observations

Here, we apply an gHK model to a spatial image of wind speed magnitude from hurricane Sandy ([www.nhc.noaa.gov/data](http://www.nhc.noaa.gov/data)), observed in October 2012 (fig. 4). As a start point for the estimation of the climacogram, autocovariance and variogram, we choose the center of the image in fig. 4b (which has 0 wind speed as it is the eye of the hurricane) and not an arbitrary point (usually is the bottom left), which would cause high anisotropy.

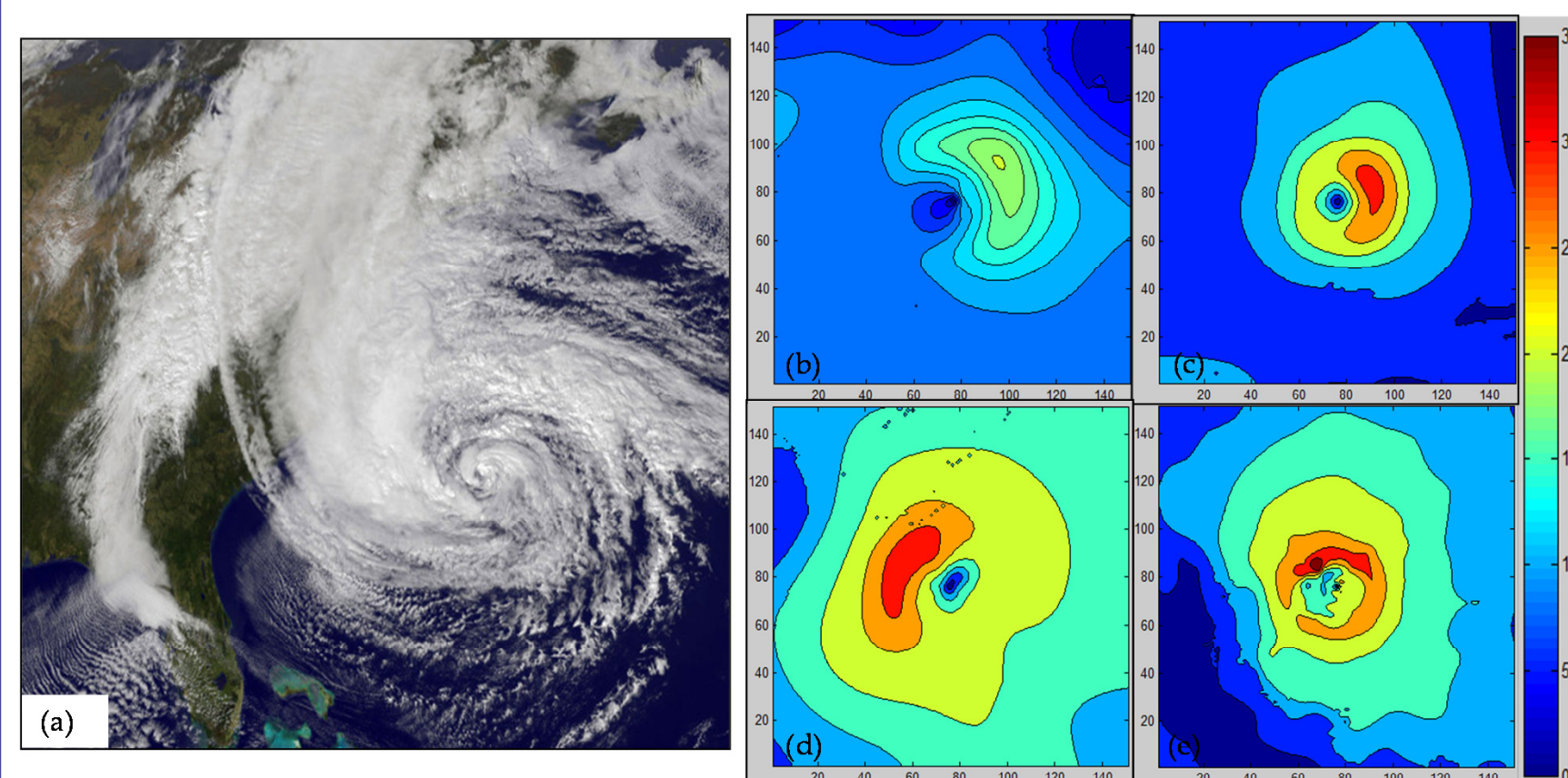


Figure 4: The image on the right (a) shows the Sandy hurricane from a satellite view (source: [www.nhc.noaa.gov/data](http://www.nhc.noaa.gov/data)), on which wind velocity and directions measurements are based. The left images, represent the wind speed magnitude (in m/s) across a 150 X 150 grid (the distance between two points is 10 km) centralized to the eye of the hurricane observed in the 23<sup>rd</sup> (b), 25<sup>th</sup> (c), 27<sup>th</sup> (d) and 29<sup>th</sup> (e) of October 2012.

## 9. Hurricane wind speed observations (cont.)

Here, anisotropy is apparent (high dispersion of observed data). Here, we ignore this and fit the average stochastic structure of the hurricane wind magnitude. The fitted parameters for each date (fig. 6) are used to incorporate time in the gHK model (i.e. creating a 2D\* spatiotemporal model).

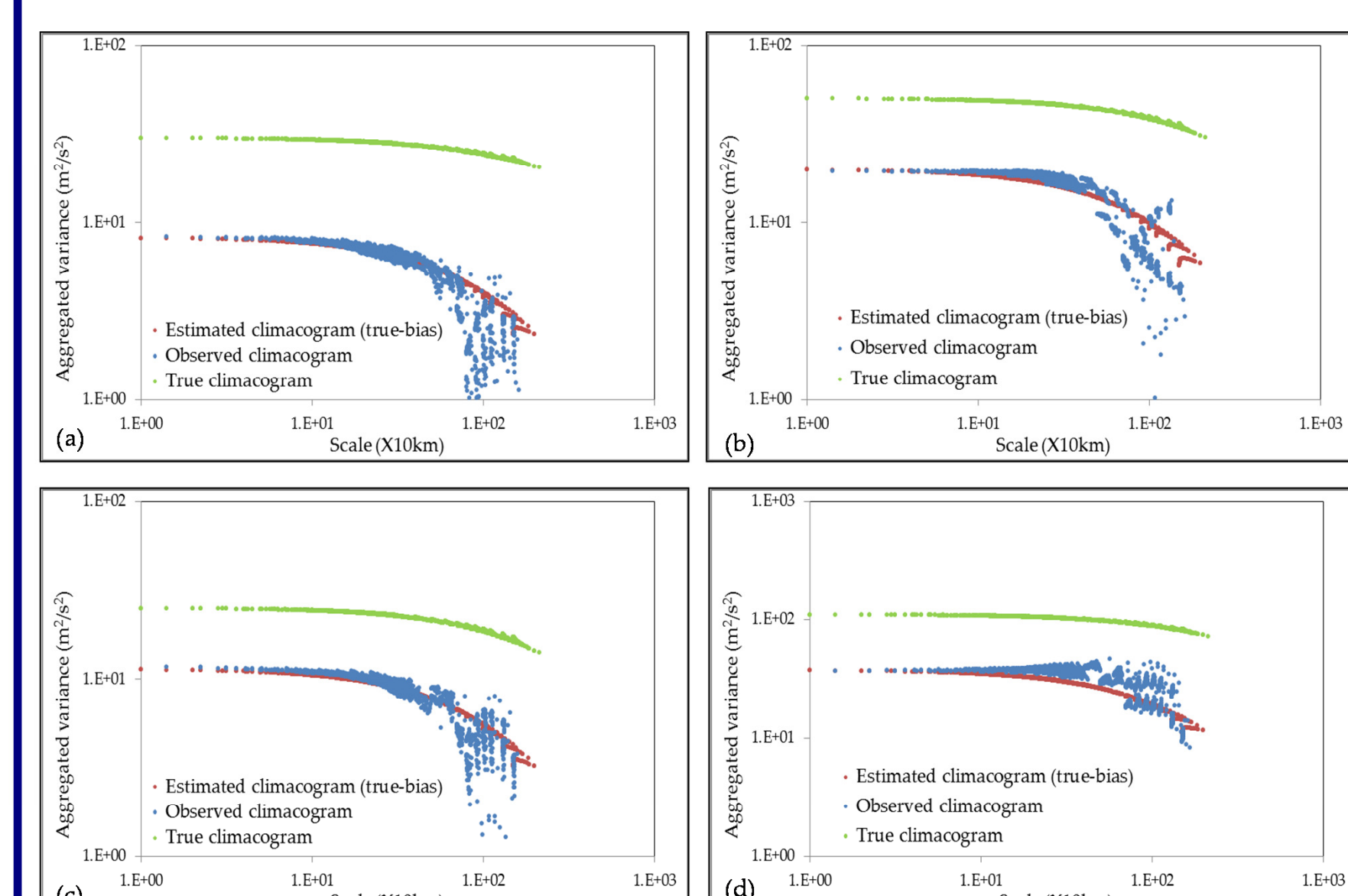


Figure 5: Climacograms for the 23<sup>rd</sup> (a), 25<sup>th</sup> (b), 27<sup>th</sup> (c) and 29<sup>th</sup> (d) day of October 2012.

## 10. Hurricane wind speed observations (cont.)

This gHK model does not provide spatiotemporal cross-covariances with time lag greater than 0 and scales greater than 1. Note that the observed temporal autocorrelations are estimated around  $0.5 \pm 0.1$  for all time lags, i.e. not varying much.

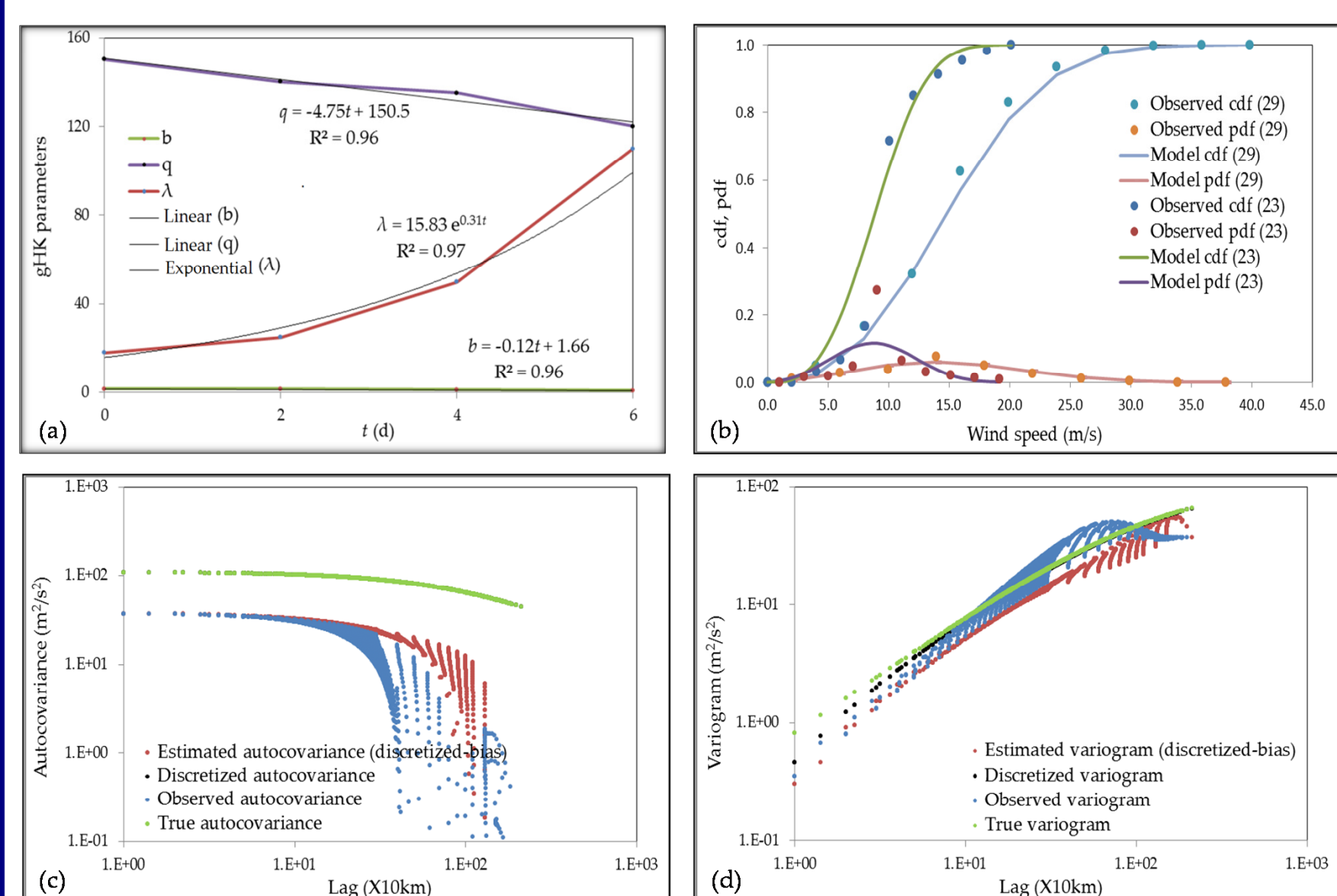


Figure 6: gHK parameters estimations vs time ( $t$ ) (a), fitted Weibull positively skewed cdf and pdf for the 23<sup>rd</sup> and 29<sup>th</sup> (b), autocovariances (c) and variograms (d) for the 29<sup>th</sup> of October.

## 11. Simulated fully developed turbulence

Here, we apply an gHK model to a 2D spatial simulation of fully developed turbulence provided by INSIDE ([http://inside.hlr.de/hum/Edition\\_01\\_11/article\\_09.html](http://inside.hlr.de/hum/Edition_01_11/article_09.html)). The parameters are estimated as:  $\lambda=0.016$  m/s,  $q=1$  m and  $b=0.2$  ( $H=0.95$ ).

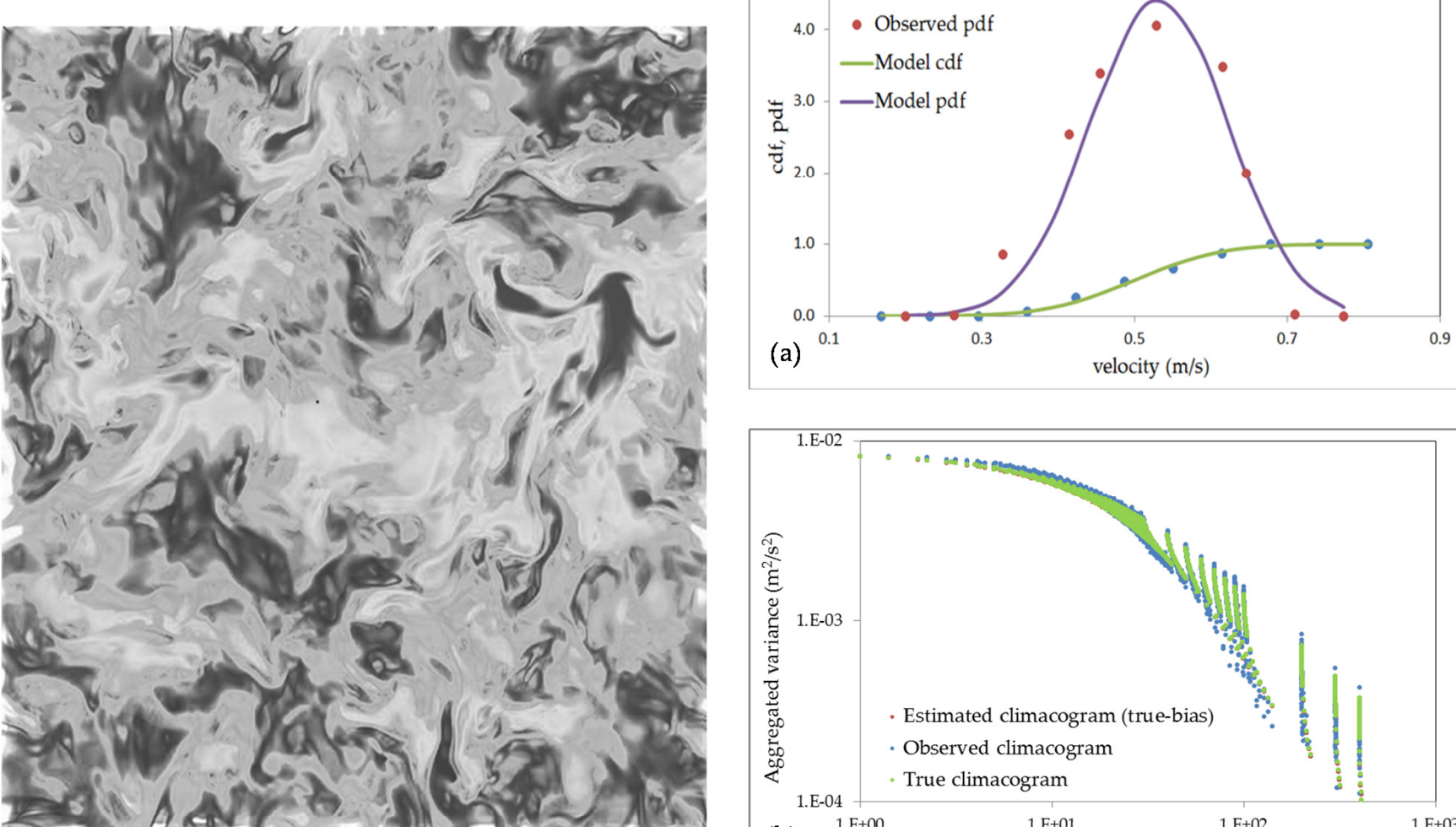


Figure 7: Grayscale image of simulated fully developed turbulence produced from the vorticity formulation of the incompressible Navier-Stokes equation with 5123 grid points. Figure 8a: Fitted Gaussian cdf and pdf (a) and climacogram (b) of the fully developed turbulence simulation image of fig. 6.

## 12. Simulated fully developed turbulence (cont.)

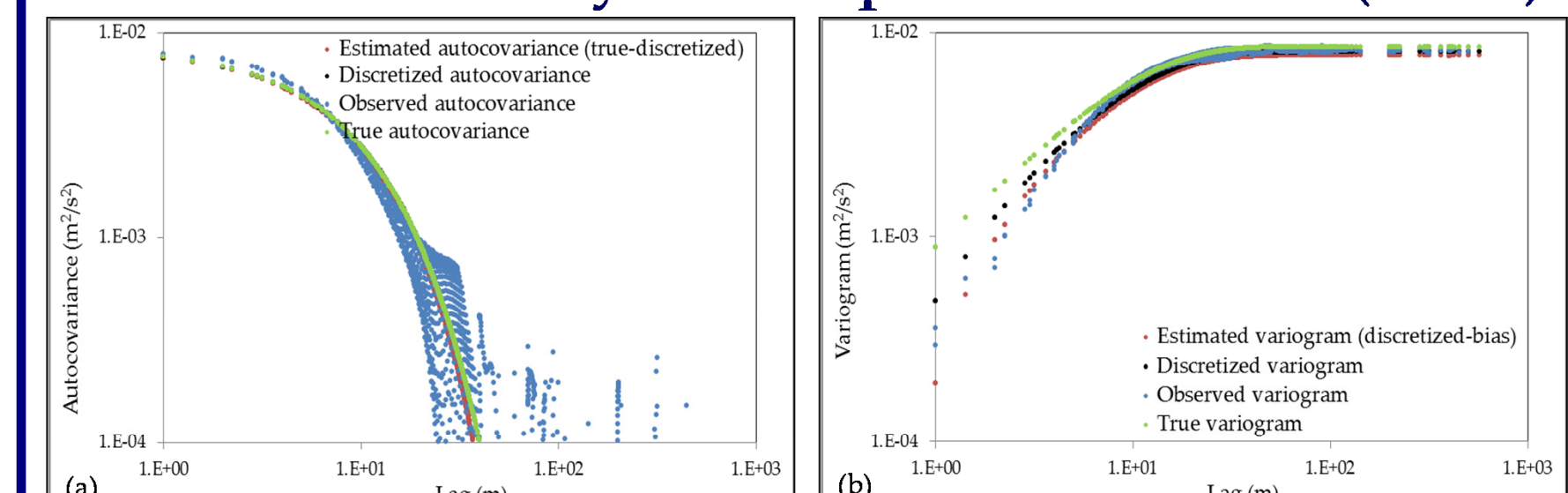


Figure 8b: Autocovariance (a) and variogram (b) of the fully developed turbulence simulation image of fig. 6.

## 13. Conclusions-Comments

From the above investigations we can see that, based on the models used, the Hurst coefficient  $H$  is relatively high (above 0.7 in most cases) in the above 2D coloured images of turbulent wind structures in large scales (ch. 6), intermediate ones (ch. 8) as well as small ones (ch. 11), indicating the clustering of colours of similar intensity, i.e. a long-term structure. Similar values of  $H$  for turbulent processes have been estimated by others (e.g. Dimitriadis and Koutsoyiannis, in preparation, Helland and Van Atta, 1977). Also, the Gaussian distribution seems appropriate only in the small scale case whereas for higher scales distributions are highly skewed.

References  
 Dimitriadis, P. and D. Koutsoyiannis, Power spectrum and autocovariance vs climacogram in stochastic modelling, in publication.  
 Dimitriadis, P., D. Koutsoyiannis and C. Onof, Multi-dimensional stochastic modelling, in publication.  
 Helland, K.N. and C.W. Van Atta, The 'Hurst phenomenon' in grid turbulence, *J. Fluid Mechanics*, 83(3), pp. 573-589, 1978.  
 Koutsoyiannis, D., A. Paschalis and N. Theodoratos, Two-dimensional Hurst-Kolmogorov process and its application to rainfall fields, *Journal of Hydrology*, 398 (1-2), 91-100, 2011.  
 Koutsoyiannis, D., Encopion of stochastic: Fundamentals of stochastic processes, 12 pages, Department of Water Resources and Environmental Engineering - National Technical University of Athens, Athens, 2013.  
 Perri S., M.L. Goldstein, J. C. Dorelli and F. Sahrarov, Detection of Small Scale Structures in the Dissipation Regime of Solar Wind Turbulence, *PhysReel.Lett.*, 109 (19), 2012.